

Wave modulation and breakdown

By W. K. MELVILLE

R. M. Parsons Laboratory, Massachusetts Institute of Technology, Cambridge, MA 02139
and Institute of Geophysics and Planetary Physics, University of California, San Diego,
La Jolla, CA 92093

(Received 6 October 1981 and in revised form 7 September 1982)

Time series of amplitude, frequency, wavenumber and phase speed are measured in an unstable deep-water wavetrain using a Hilbert-transform technique. The modulation variables evolve from sinusoidal perturbations that are well described as slowly varying Stokes waves, through increasingly asymmetric modulations that finally result in very rapid jumps or 'phase reversals'. These anomalies appear to correspond to the 'crest pairing' described by Ramamonjiarisoa & Mollo-Christensen (1979). The measurements offer a novel local description of the instability of deep-water waves which contrasts markedly with the description afforded by conventional Fourier decomposition. The measurements display very large local modulations in the phase speed, modulations that may not be anticipated from measurements of the phase speeds of individual Fourier components travelling (to leading order) at the linear phase speed (Lake & Yuen 1978).

1. Introduction

The last two decades have seen considerable theoretical advances in our knowledge of the stability and interactions of nonlinear waves (see Whitham 1974; and, for a recent personal account, Phillips 1981*a*). It is well known that such phenomena lead to modulations of wavenumber and frequency, as well as amplitude, with the frequency dependent on both wavenumber and amplitude. These modulations are not just theoretical curiosities but have important consequences in oceanography and meteorology, as well as naval architecture and ocean engineering (Longuet-Higgins 1980).

Despite these theoretical advances the experimental measurement of these modulations has lagged far behind and I know of no published method in the fluid-mechanics literature that demonstrates an unambiguous simultaneous measurement of both amplitude and phase modulation. However, the basis of such a method has existed in the communications and electrical-engineering literature for the same two decades and is developed here to demonstrate the method on surface gravity waves.†

In one of the first experimental papers on the stability of nonlinear gravity waves, Feir (1967) used the measured time between crests to show the frequency modulation that accompanies amplitude modulation. Unfortunately this gives a rather poor resolution of the frequency, which is adequate only for slowly modulated wavetrains. Subsequent workers in the field have used rectification and low-pass filtering of the surface displacement to provide a measure of amplitude modulation, and zero-crossing methods to measure frequency modulation (Lake & Yuen 1978). However, such

† Since this work was informally reported and this paper begun, a thesis with preliminary results for wind waves has appeared (Sahar 1981).

methods are not reliable when the wave amplitude undergoes very large fluctuations in one wave period. Conclusions based on such methods of data analysis are also questionable. Much of the data analysis relating to wave stability has depended on power-spectral estimates (Lake *et al.* 1977; Melville 1981) in which the phase information is neglected entirely. Moreover the spectra may become rapidly populated with numerous discrete lines (along with a continuous spectrum), rendering simple interpretations difficult, if not impossible.

The work reported here was originally motivated by the need to compare fluid velocities and phase velocities in breaking waves (Melville 1982). We originally intended to use the conventional correlation between two wave gauges to obtain the phase speed of the waves. However, it was soon realized that such measurements are global in that they represent phase speeds of Fourier components obtained from time series of considerable duration, whereas the breaking events are local in time and spread over a number of Fourier components. Initial measurements also showed that significant frequency modulations could occur in a mechanically generated wavetrain of initially uniform frequency, so there was no reason to expect that an unstable wavetrain could be characterized by a single wavenumber or phase speed. These observations do not agree with a conjecture of Lake & Yuen (1978) that the numerous Fourier components in a strongly modulated mechanically generated wavetrain were not free waves but merely the bound components needed to describe the individual waves and their envelope. This conjecture was used to interpret wind-wave data in which the effects of nonlinearity dominated those of randomness.

The validity of the linear or weakly nonlinear dispersion relationship in wind-wave fields has been questioned by a number of workers since Ramamonjariisoa's (1974) laboratory measurements. Some of the ambiguities involved in measuring the component wave speeds have been recently resolved by Phillips (1981*b*) and Crawford *et al.* (1981). While this question is not directly addressed here, the controversy regarding the phase speed of surface waves indicated that it was not generally appreciated that the local phase speed could be accurately measured as a function of time; with most experimenters resorting to measuring the phase speed of the individual Fourier components.

In this paper we show, with some relatively weak restrictions, that the measurement of the surface displacement can be used to obtain the time series of both amplitude and phase at a point. Finite-differencing of the phase in space and time leads to time series of wavenumber and frequency respectively, and hence the phase speed. The method is demonstrated on nonlinear deep-water waves. It confirms the dispersion relationship to $O(\epsilon^2)$ for weakly modulated waves, and shows evidence of anomalous behaviour in the phase with very rapid variations of the wavenumber, frequency and phase speed. This phenomenon which appears as a phase reversal may be related to the 'crest pairing' of Ramamonjariisoa & Mollo-Christensen (1979) and the 'lost' wave crests of Lake & Yuen (1978). The amplitude and frequency records are used to measure a propagation speed for these modulations. These results suggest that the description of such strongly modulated mechanically generated wavetrains as being 'effectively non-dispersive' (Lake & Yuen 1978) may need reassessment.

In §2 the method for retrieving the amplitude and phase is presented. In §3 the experiments are described. The results are given in §4, and their interpretation discussed in §5.

2. Modulation measurement

The basis of the method for measuring the amplitude and phase depends on the use of the Hilbert transform to represent the complex part of an analytic signal whose real part is measured. The method has been used in the electrical-engineering literature in the context of signal demodulation for at least two decades (Schwartz, Bennett & Stein 1966; Deutsch 1962; Bracewell 1978). The novelty of its use here lies in the demonstration that not only frequency modulation but also wavenumber modulation, and hence phase-speed modulation, can be measured.

If $g(t)$ is a real function of time in the interval $-\infty < t < \infty$ we may define the *analytic function*

$$h(t) = g(t) - i\hat{g}(t), \quad (2.1)$$

where

$$\hat{g}(t) \equiv \frac{1}{\pi} \mathcal{P} \int_{-\infty}^{\infty} \frac{g(t') dt'}{t' - t}, \quad (2.2)$$

is the Hilbert transform of g . From the convolution theorem,

$$\mathcal{F}(\hat{g}) = i \operatorname{sgn} s \mathcal{F}(g), \quad (2.3)$$

where \mathcal{F} denotes the Fourier transform. It follows that

$$\mathcal{F}(h) = 2\mathcal{F}(g) \quad (s \geq 0), \quad (2.4a)$$

$$= 0 \quad (s < 0). \quad (2.4b)$$

Use of (2.4) and the fast-Fourier-transform algorithm makes computation of $h(t)$ fast and efficient.

From the above results it follows that if

$$g(t) = \mathcal{R}[a(t) e^{i\phi(t)}] \quad (2.5)$$

then

$$h(t) = a(t) e^{i\phi(t)}. \quad (2.6)$$

The analytic function then describes both amplitude and phase modulation. In particular, from (2.6) we may define a wave field by a 'carrier' frequency σ_0 and a complex envelope $A(t)$, where

$$h(t) = A(t) e^{-i\sigma_0 t}, \quad (2.7)$$

$$A(t) = a(t) e^{i(\phi + \sigma_0 t)}. \quad (2.8)$$

This description is constrained by the requirement that the bandwidth of the spectrum of $A(t)$ be less than or equal to $2\sigma_0$ (Schwartz *et al.* 1966).

In the nonlinear surface waves of interest the spectrum is populated in the neighbourhood of the fundamental frequency and the higher harmonics. It is therefore necessary to bandpass the measured signal to satisfy the bandwidth constraint on $A(t)$. This is the only arbitrary step in the procedure outlined here, and in all the results presented the frequency bands are defined by $\sigma_0(n - \frac{1}{2}, n + \frac{1}{2})$, $n = 1, 2, \dots$, where σ_0 is the fundamental frequency. It should be stressed that this filtering (in Fourier space) does not necessarily restrict the instantaneous frequencies to these bands.

This bandpass filtering also fits quite naturally (as it should) with theoretical descriptions which describe the wave field as an ordered series of functions representing the modulation of the fundamental wave and its harmonics. For example, if

$$\eta(x, t) = \mathcal{R} \sum_j e^j a_j e^{i\phi_j} \quad (j = 0, 1, 2, \dots)$$

represents the surface displacement with the j th term representing the contribution from the neighbourhood of the $(j+1)$ th harmonic, with ϵ as the (small) ordering parameter, then the amplitude a_j and phase ϕ_j can be evaluated. The wavenumber and frequency defined respectively by

$$k_j(x, t) = \frac{\partial \phi_j}{\partial x}, \quad \sigma_j(x, t) = -\frac{\partial \phi_j}{\partial t},$$

may be approximated by the appropriate first differences.

In the experiments described below, time series of surface displacement were measured at time intervals of Δt at two stations separated by a small distance Δx in the direction of wave propagation. Each time series was Fourier-transformed and bandpass filtered, and the analytic signal was computed and decomposed into its polar components a and ϕ . The amplitude, frequency, wavenumber and phase speed were then estimated by

$$\begin{aligned} a(x, t) &= \frac{1}{2}[a(t; x - \frac{1}{2}\Delta x) + a(t; x + \frac{1}{2}\Delta x)], \\ \sigma(x, t) &= [\phi(t - \frac{1}{2}\Delta t; x) - \phi(t + \frac{1}{2}\Delta t; x)]/\Delta t \\ k(x, t) &= [\phi(t; x + \frac{1}{2}\Delta x) - \phi(t; x - \frac{1}{2}\Delta x)]/\Delta x \\ c(x, t) &= \sigma/k \end{aligned}$$

respectively.

3. The experiments

The technique was tested during a series of experiments that have been described at some length in a recent paper (Melville 1982) and the reader is referred there for the detail not given here.

The experiments were conducted in the glass channel at the Hydraulics Laboratory, Scripps Institution of Oceanography. The channel is 0.5 m wide, 28 m long and the water was 0.6 m deep. Uniform deep-water 2 Hz waves were mechanically generated at one end of the channel and became unstable through the Benjamin–Feir mechanism, which led ultimately to breaking. The waves were dissipated on a beach at the other end of the channel.

Surface-displacement measurements were made with two resistance wave gauges separated by 8 cm (Δx) in the direction of wave propagation. The wave gauges were sampled at 100 Hz in the unbroken wave field at 200 Hz in the breaking region. The data were stored on magnetic tape and processed on a digital computer.

The calibrated data were bandpass-filtered in bands of 2 Hz width centred on the fundamental frequency (2 Hz) and its higher harmonics. The analytic functions were subsequently computed for each of these filtered signals. Three series of experiments were processed in this manner for $0.23 \leq ak \leq 0.29$,† only one series of experiments ($ak = 0.23$) was examined in the detail presented below. However, the results for $ak = 0.29$ agree in all important physical respects with these results.

The position of the measurements in the data presented below is described by the

† The amplitude here refers to the amplitude of the initial uniform wavetrain and is defined as half the difference between the mean crest and mean trough position sampled over 100 waves. This amplitude includes contributions from all the Fourier components. This should not be confused with the amplitude of the first term in the Stokes' expansion.

dimensionless distance xk_ℓ , where x is the distance down the channel from the equilibrium paddle position and k_ℓ (0.161 cm^{-1}) is the wavenumber of the linear deep-water wave of 2 Hz.

4. Results

4.1. Single-point measurements

Figure 1(a) displays the essentially uniform wavetrain at $xk_\ell = 58$, the displacement η_0 from Fourier components in the fundamental band (1–3 Hz), the amplitude $a_0(t)$, the phase $\phi_0(t)$ and the frequency $\sigma_0(t)$. The measured amplitude in the fundamental band is almost constant and is, to the accuracy of the experiment, equal to the total wave amplitude. This is to be expected, since the first correction to the wave amplitude in the Stokes expansion is of order $(ak)^2$, comparable to the expected measurement error.† The measured frequency differs by at most 1% from that of the 2 Hz sinusoidal waveform driving the wave generator.

Figure 1(b), at $xk_\ell = 155$, shows the modulated wavetrain resulting from the Benjamin–Feir instability, with both amplitude and frequency modulations present. At this station the modulations are approximately sinusoidal. However, at $xk_\ell = 177$ (figure 1c) the frequency modulation is beginning to show an asymmetric form with steeper forward faces and more gently sloping rear faces. At this station the waves were occasionally breaking. Figure 1(d) ($xk_\ell = 209$, in the established-breaking region), shows the further development of the asymmetry, with the amplitude modulations also showing steep forward faces. The frequency modulation now shows an asymmetry in amplitude (i.e. about the initial frequency of 2 Hz) as well as in time: the positive perturbations are significantly greater than the negative perturbations. The positive-frequency perturbations have also extended beyond the upper limit of the bandpass filter (3 Hz); presumably a consequence of the nonlinear interaction between different Fourier modes in the fundamental band. The results at $xk_\ell = 242$

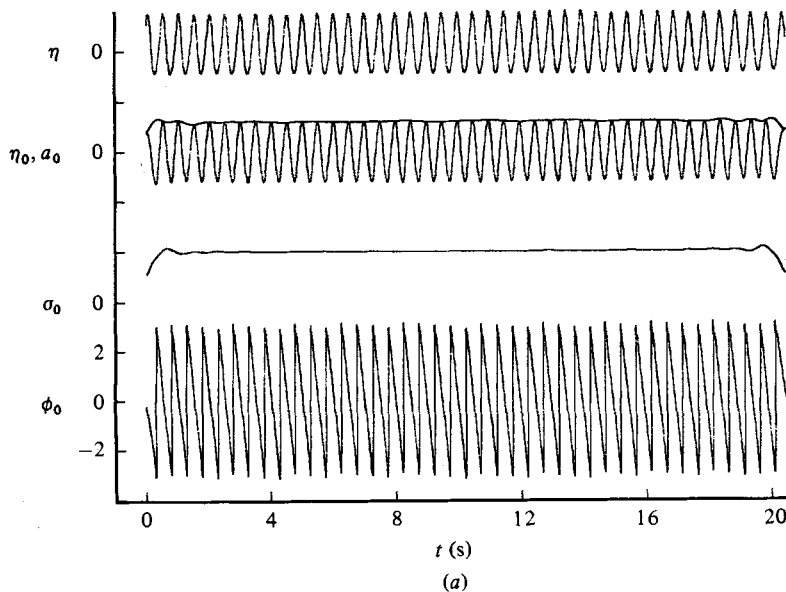


FIGURE 1(a). For caption see p. 495.

† Experimental errors are discussed in the appendix.

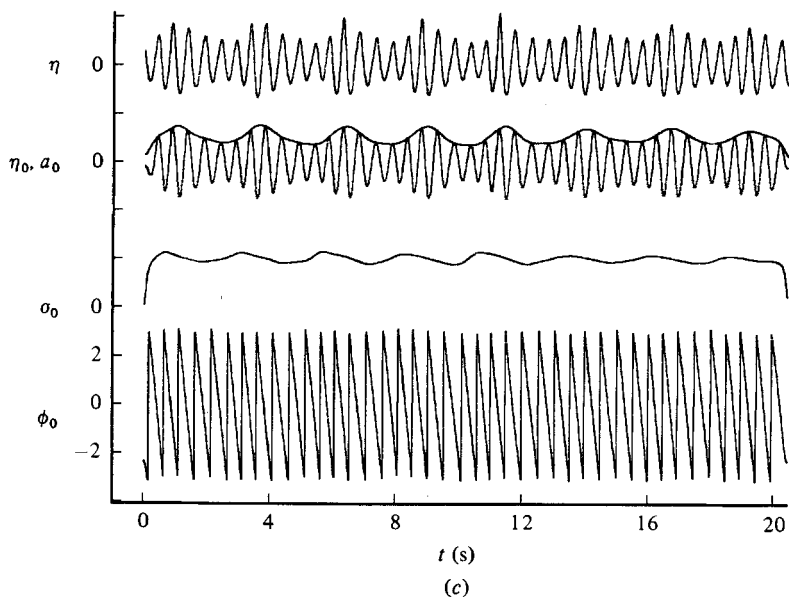
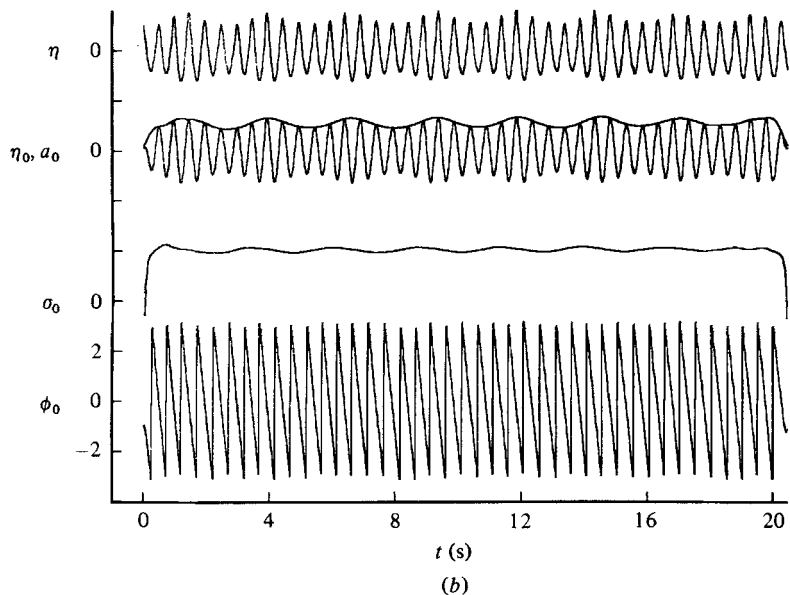


FIGURE 1 (*b, c*). For caption see facing page.

(figure 1 *e*) show a dramatic change, with the amplitude modulations extending almost to zero with small coincident regions of negative frequency. These negative frequencies result from regions of phase reversal. They will be examined in more detail in §4.3. The other important process displayed in this figure is the evolving phase shift between the amplitude and frequency modulations. In figure 1 (*a*) the frequency leads the amplitude by approximately 90° , consistent with the linear analysis of the Benjamin–Feir instability. As the waves evolve down the channel the phase difference increases until (in figure 1 *d*) the amplitude and frequency are approximately 180° out of phase.

Similar processing may be carried out on the second-harmonic band covering

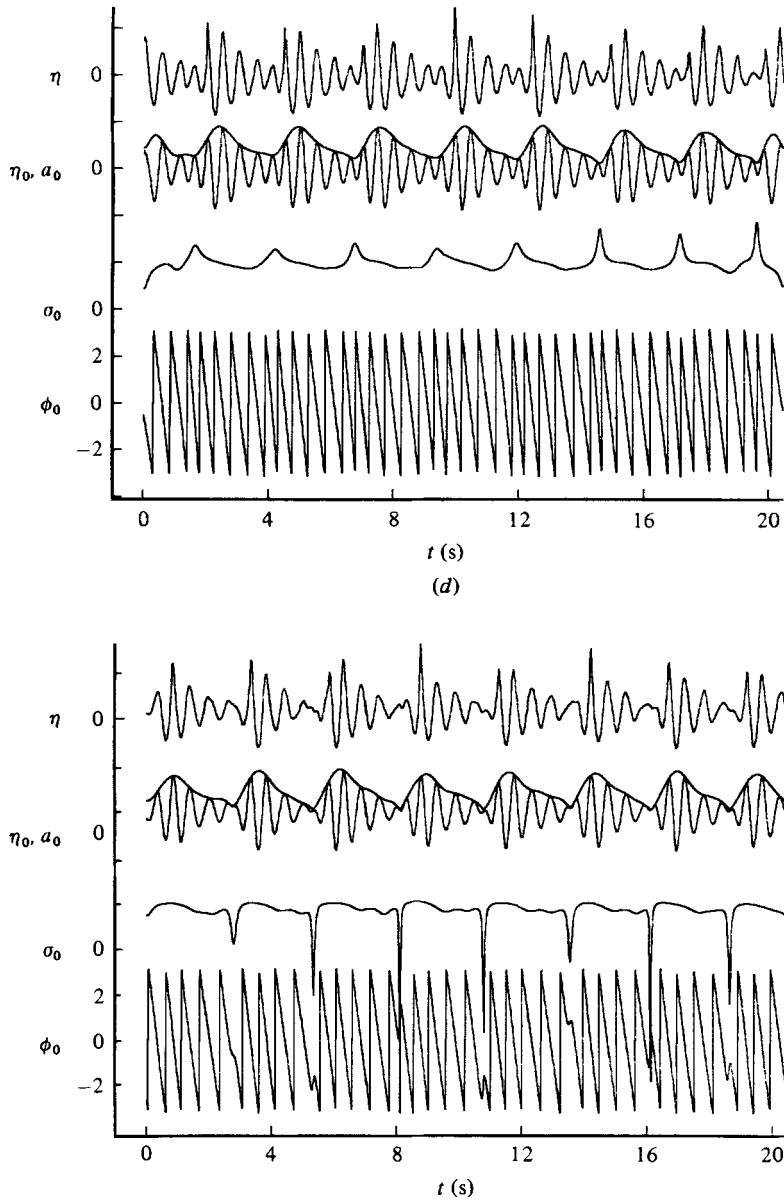


FIGURE 1. Surface displacement η , bandpassed (1–3 Hz) displacement η_0 , amplitude a_0 , frequency σ_0 and phase ϕ_0 at (a) $xk_L = 58$; (b) 155; (c) 187; (d) 219; (e) 251.

frequencies in the range 3–5 Hz, and the results are shown in figures 2(a–c). Each of these figures shows the unfiltered wavetrain, the filtered wavetrain and the corresponding amplitude, phase and frequency signals. Figure 2(a) ($xk_L = 155$, cf. figure 1b) shows evidence of more than one modulation frequency, which when compared with figure 1(b), at the same station, clearly shows that the waves are not simply modulated Stokes waves. In figure 2(b) ($xk_L = 177$) we already see evidence of the phase reversals, not seen until $xk_L = 242$ in the fundamental band. In addition there are large positive-frequency perturbations with frequencies greater than 10 Hz, or more than double the largest Fourier-component frequency in this band. Further,

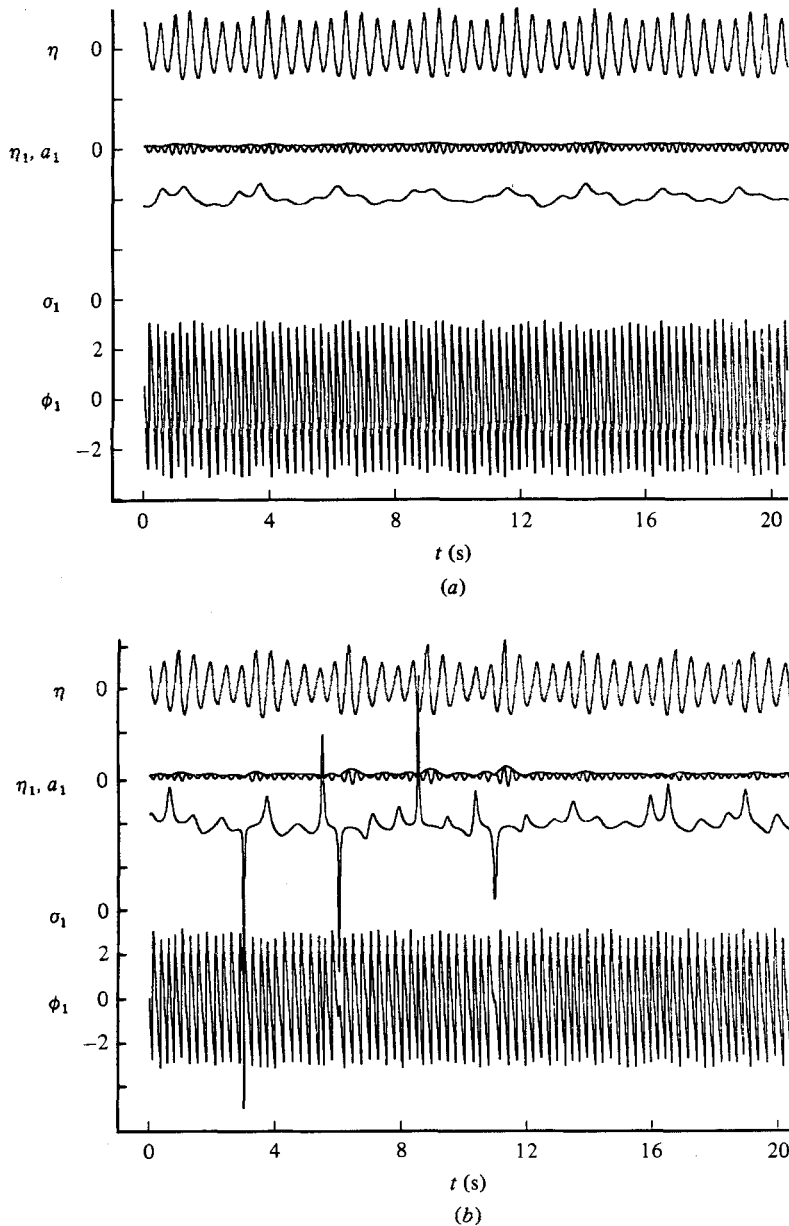


FIGURE 2(a, b). For caption see facing page.

the frequency perturbations also extend below into the fundamental-frequency band. Figure 2(c) shows the second-harmonic band at $xk_l = 242$, where again the instantaneous frequencies extend above and below the range 3–5 Hz. The amplitude has become localized in the neighbourhood of the largest waves, contributing to the asymmetry of the wave groups that is apparent in the surface-displacement signal.

4.2. Two-point measurements

The single-point measurements do not permit a resolution of the wavenumber. This may be resolved with two adjacent measurements, which in this case was accomplished

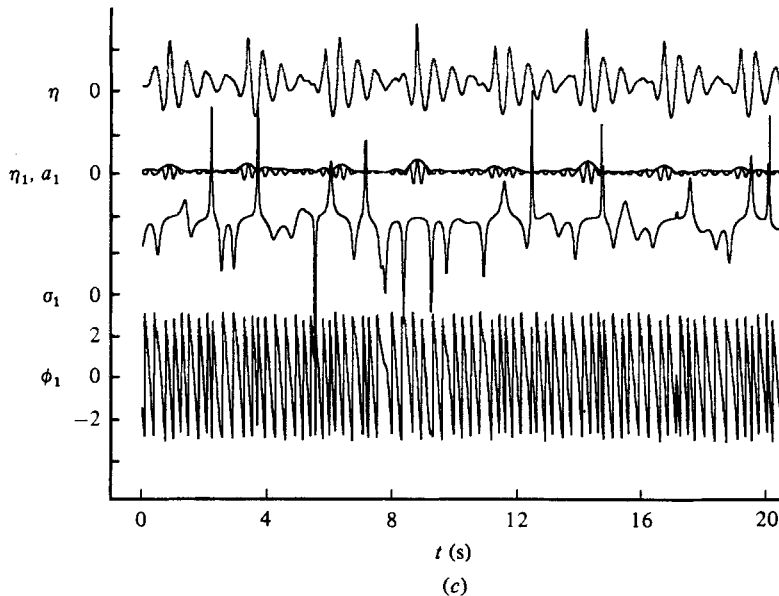


FIGURE 2. Surface displacement η , bandpassed (3–5 Hz) displacement η_1 , amplitude a_1 , frequency σ_1 and phase ϕ_1 at (a) $xk_\ell = 155$; (b) 187; (c) 251.

by two wave gauges separated by a distance of 8 cm in the direction of wave propagation. This separation proved small enough to resolve quite accurately the wavenumber modulations of the fundamental band. Measurements made with a separation of 1.5 cm gave unacceptable errors in the measured wavenumber. The cause of these errors was not determined, but it may be mechanical (e.g. wake interference) or electronic (interference between the two bridges). As a result, the wavenumber measurements were restricted to the fundamental band for which the wave-gauge separation was a sufficiently small fraction of the wave length: approximately 0.2 of the uniform wavetrain.

Figures 3(a–d) show the wavenumber k_0 (cm^{-1}), the frequency σ_0 (Hz), the slope $a_0 k_0$ (based on the amplitude of the envelope of the fundamental band), and the measured and theoretical phase speed normalized by the linear phase speed for 2 Hz waves. † The measured phase speed c was computed from the measured frequency and wavenumber. The theoretical phase speed c_t was computed from the approximate dispersion relationship

$$\sigma_0^2 = gk_0[1 + (a_0 k_0)^2] \quad (4.1)$$

using the *measured* wavenumber k_0 and *measured* amplitude a_0 . For consistency an additional correction proportional to the second spatial derivative of the amplitude should be included for strongly modulated waves (Chu & Mei 1970); however this would have required a third displacement measurement for finite differencing.

Unfortunately the data taken at the station closest to the paddle were not usable and so no direct check of the dispersion relationship for the unmodulated wavetrain was possible. However, figure 3(a) ($xk_\ell = 155$) shows an approximately sinusoidal modulation of all the variables with a very good agreement between the measured

† This unlikely combination of dimensioned and dimensionless variables was chosen for ease of graphical representation.

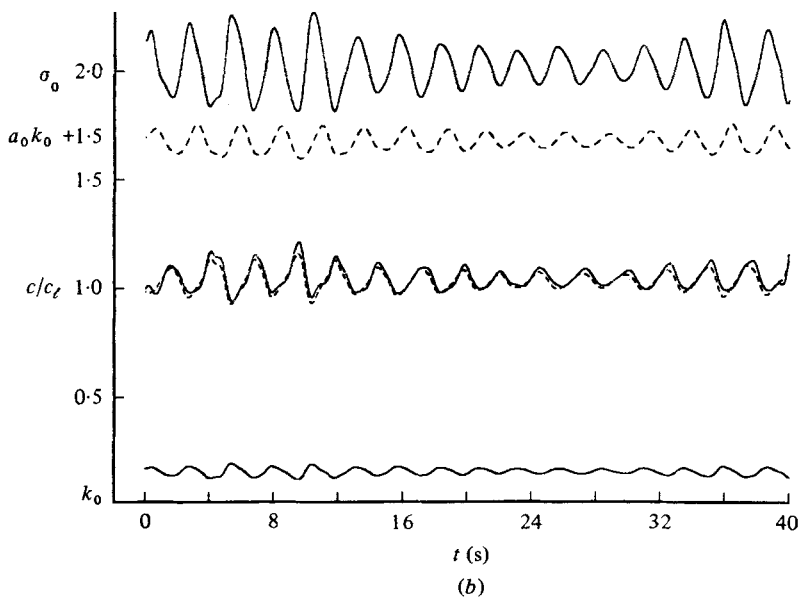
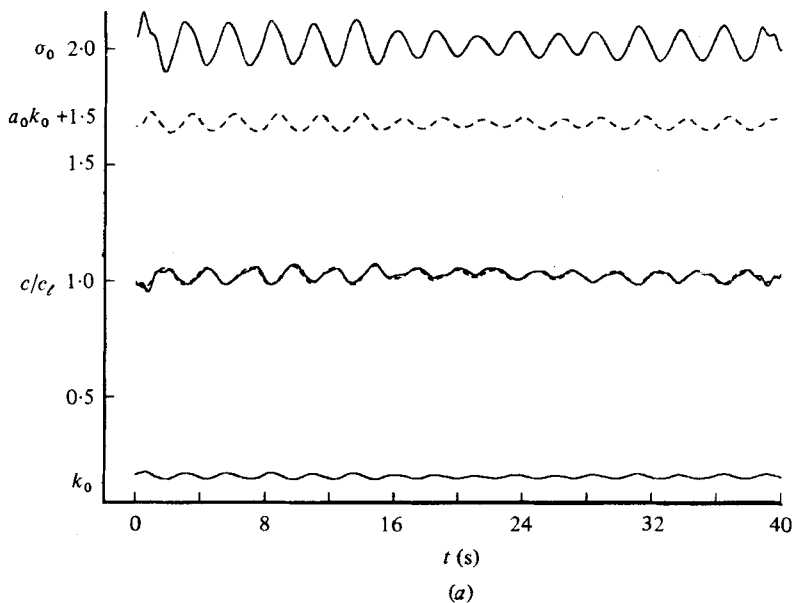


FIGURE 3(a, b). For caption see facing page.

and theoretical phase speeds. The difference between these two speeds is at most 1% in this weakly modulated wavetrain. Longer-period fluctuations are also evident and are most likely evidence of long period modes of the channel. These are also seen in figure 3(b) ($xk_z = 187$), where the waves were occasionally breaking. This intermittent breaking is almost certainly due to these longer-period fluctuations. The important features of this figure are the good agreement between the phase speeds, and the development of asymmetry in the wavenumber fluctuations. The wavenumber and frequency fluctuations are in phase and lead the slope fluctuations. No accurate measure of this phase difference was made, but it appears to be in the range $[\frac{1}{4}\pi, \frac{1}{2}\pi]$.

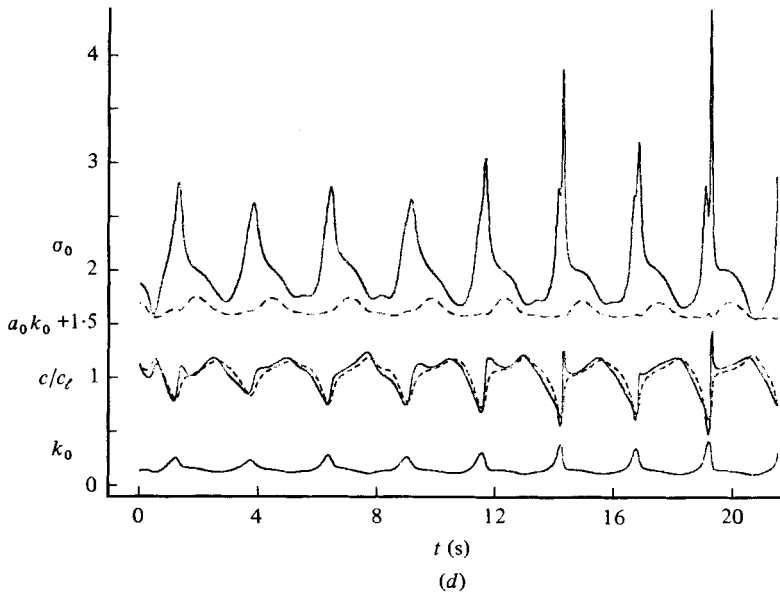
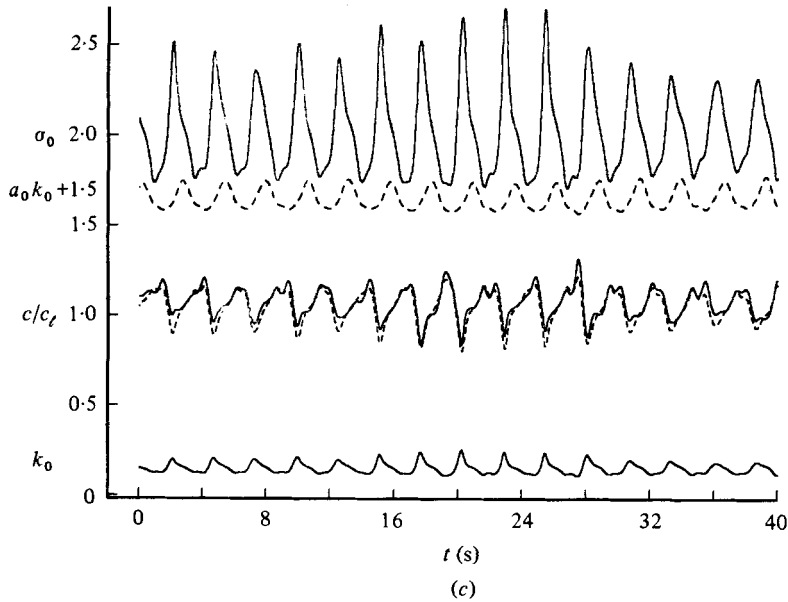


FIGURE 3. Fundamental modulation variables: wavenumber k_0 (cm^{-1}), measured phase speed c/c_L (—), computed phase speed c_t/c_L (---), $a_0 k_0 + 1.5$ and frequency σ_0 (Hz) at (a) $xk_L = 155$; (b) 188; (c) 204; (d) 220.

Figure 3(c) ($xk_L = 204$) displays measurements from the established-breaking region. The agreement between the phase speeds is still quite good, although the errors at the extrema are now as large as $\pm 9\%$, with maxima as much as 32% greater than the linear phase speed, and minima as much as 17% less. The measured wavenumber is now showing strong asymmetries in both amplitude and time, which are also evident in the frequency. The slope curves have begun to develop sharper crests than troughs but remain approximately symmetric in time.

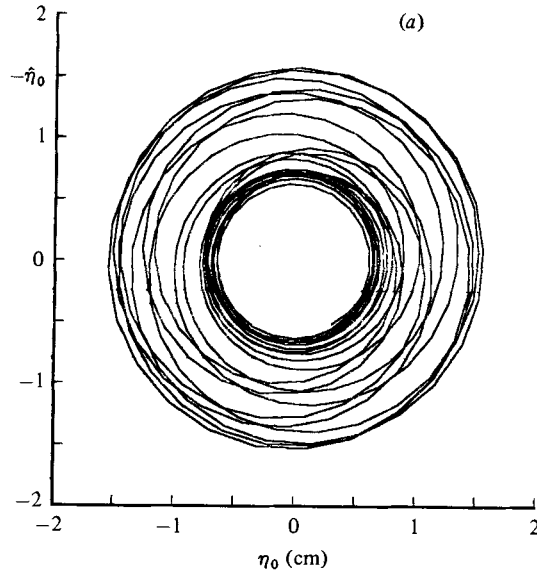


FIGURE 4(a). For caption see facing page.

The final figure in this series (figure 3(d), $xk_\ell = 220$) shows that the perturbation in wavenumber and slope have become localized within each group. The frequency (which is linearly interpolated between the two gauges) is changing so rapidly in space that the finite separation of the gauges may be evident in the last few groups. The agreement between phase speeds is still remarkably good, with the exception of the regions in which the frequency is rapidly changing. Immediately following this record (at the same station) phase reversals were measured and gave rise to rapid jumps in the measured variables. These jumps were also evident at the final station ($xk_\ell = 252$). They are examined in more detail in §4.3.

4.3. Phase reversals

The most surprising aspect of these results is the appearance of phase reversals. They occur first in the second-harmonic band and then in the fundamental band at a station further downstream. The resolution of the phase is best shown in a polar diagram of the trajectory of $(a_0(t), \phi_0(t))$ where the real axis is the measured, filtered, surface displacement, and the imaginary axis its Hilbert transform.

Figure 4(a) (cf. figure 1) shows such a trajectory at $xk_\ell = 204$ for a period of 10 s. The trajectory is contained in an annular region described by the maxima and minima of the envelope. (For a uniform wavetrain the trajectory describes a circle centred at the origin with a radius equal to the envelope amplitude.) It is worth noting that the trajectory passes around the origin, the phase decreases monotonically by 2π in each (not necessarily equal) wave period, so that the frequency is everywhere positive. However, at $xk_\ell = 251.38$ (figure 4(b), cf. figure 1) we see that the trajectory on four occasions does not pass around the origin, but instead forms a closed loop in the neighbourhood of the origin. That is, the phase does not decrease monotonically but *increases* in a small interval of time during which the amplitude is also small. Figure 4(c) shows the trajectory at $xk_\ell = 252.67$ over the same period displayed in figure 4(b), and here we see that the anomalies in the trajectory have evolved (in just 8 cm), with the loops disappearing, leaving regions of large curvature in the trajectory. These anomalies are clearly evolving rapidly; changing qualitatively in a small distance as they propagate in the same direction as the waves.

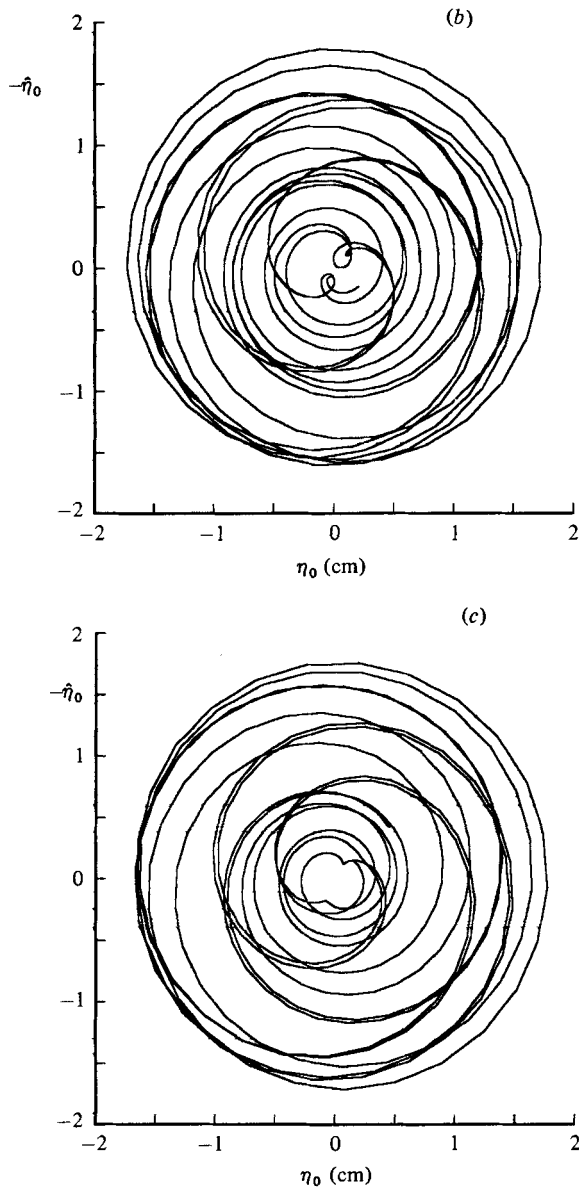


FIGURE 4. Polar diagram of the analytic function $h_0(t) = \eta_0(t) - i\hat{\eta}_0(t)$ at (a) $xk_t = 203$; (b) 251.38; (c) 252.67.

In figure 5 we have used the data at the stations shown in figures 4(b, c) to compute the variables shown earlier in figure 3. In figure 5(a) it is shown that the negative frequencies evident earlier are also accompanied by regions of negative wavenumber. These regions of negative wavenumber are coincident with very rapid changes in wavenumber. Time delays between the frequency minima at the two wave gauges were used to measure the propagation speeds of these events. The ratios of propagation velocity to linear phase speed, c_p/c_l , for the seven events in figure 5(a) are 1.01, 0.88, 1.35, 1.17, 0.91, 1.21, 1.26 respectively, with all events propagating in the same direction as the incident wavetrain. In all but the first event there existed a point where the propagation speed was equal to the local measured phase speed.

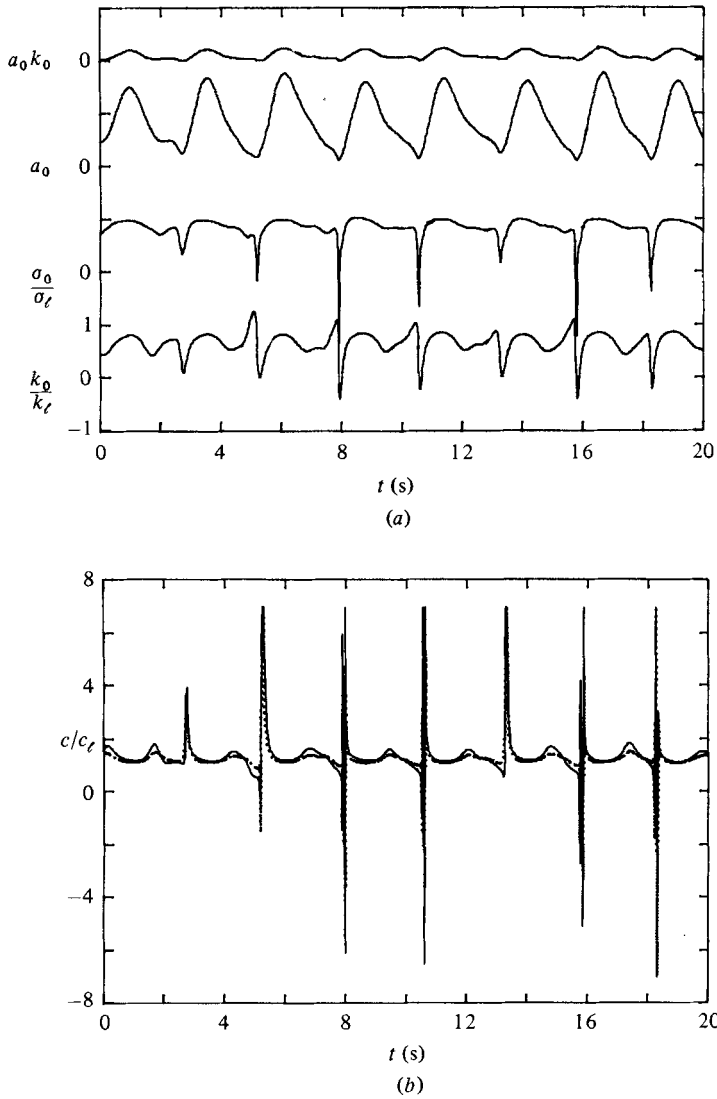


FIGURE 5. (a) Fundamental modulation variables: k_0/k_L , σ_0/σ_L , a_0 (cm), $a_0 k_0$ at $x k_L = 252$. (b) Phase speed c/c_L at $x k_L = 251$: —, measured; ..., equation (5.1).

Event	Time (s)	$c/c_{L\max}$	$c_t/c_{L\max}$	$c/c_{L\min}$	$c_t/c_{L\min}$	c_p/c_L
1	2.9	3.97	3.06	—	—	1.01
2	5.4	63.61	16.74	-0.42	-1.55	0.88
3	8.2	7.35	3.76	-6.09	-3.65	1.35
4	10.8	138.01	14.43	-6.50	-3.66	1.17
5	13.6	62.01	12.46	—	—	0.91
6	16.2	10.07	4.39	-5.11	-3.29	1.21
7	18.7	34.14	9.47	-32.47	-10.41	1.26

TABLE 1. Maxima and minima of measured and computed ratios c/c_L , c_t/c_L and measured propagation speed c_p/c_L during events in figure 5

It is worth noting that these propagation speeds are much larger than the linear group velocity of the incident wavetrain.

Figure 5(b) shows the measured and computed phase speed for the same period as shown in figure 5(a). It is evident that the regions of negative frequency and wavenumber are regions of very rapid change in the phase speed. The occurrence of negative phase speeds shows that the regions of negative wavenumber are not necessarily coincident with the regions of negative frequency. The regions of negative phase speed are very small and more accurate measurements are needed to resolve the details in these regions. Nevertheless, there appears to be reasonable qualitative agreement between the measured and computed phase speeds. (It should be noted that for ease of presentation the speeds have been arbitrarily truncated at seven times the linear value.) The maximum and minimum of the measured and computed phase speeds for each of the events in figure 5 are given in table 1. The measured maxima are as much as two orders of magnitude greater than the linear phase speed. These large variations are to be compared with the phase speed for a *uniform* wavetrain, which is at most $1.09c_g$. We do not believe that the phase speeds are accurate up to the extrema measured in each event; nevertheless, the profiles in events 1, 2 and 5 are in reasonable quantitative agreement for phase speeds up to an order of magnitude greater than the linear phase speed.

It is of interest to note that these large gradients always occur in the neighbourhood of local minima in wave amplitude. In the data processed these anomalies occurred only in the breaking region, and first in the higher harmonics.

5. Discussion

In this paper we have shown that the Hilbert-transform technique may be used to measure the amplitude, frequency, wavenumber and phase speed as continuous variables in a strongly nonlinear unsteady wavetrain. The measurements show that the weakly modulated waves in the fundamental band were consistent with the Stokes' second-order dispersion relationship. Subsequent evolution of the waves displayed features that have not been directly observed using the conventional data-analysis procedures, and are not described by available theoretical results. These include an evolving phase shift between amplitude and frequency modulations, localization of slope modulations, and phase reversals.

The initial frequency modulation was found to lead the amplitude modulation by approximately $\frac{1}{2}\pi$; but as the evolution of the groups proceeded the modulations became asymmetric and the phase difference increased to approximately π , with regions of small amplitude coincident with regions of high frequency. This suggests that amplitude and frequency modulations may have different propagation speeds. A preliminary attempt was made to determine these speeds by measuring the time required for extrema in the modulations to pass between the two wave gauges. These measurements showed considerable scatter in the range $0.3-1.2c_g$; nevertheless, at each station the mean propagation speed† for the frequency was greater than that for the amplitude (up to 30% greater), consistent with the observed change in phase shift. It is worth noting that the mean velocities were in the range 1.0–1.5 times the linear group velocity and point to the need for an examination of the use of this velocity to characterize the propagation of strongly modulated groups. Ramamonjjarisoa & Mollo-Christensen (1979) emphasized the important role of the phase

† These mean values were computed over 10–20 individual groups.

shift between amplitude and frequency modulations in describing the asymmetry between the upper and lower sidebands in the spectrum. These measurements provide initial evidence of this evolving phase shift.

The measurements also demonstrate the importance of considering wavenumber as well as amplitude modulations in determining the 'waveslope' ak (cf. Lake & Yuen 1978; Longuet-Higgins 1980). The measurements (figures 3*d*, 5*a*) display an increasing localization of ak with increasing modulation. This is reflected in the amplitude of the second-harmonic band (figure 2*c*), which also displays a coincident localization with increasing modulation. There is some evidence from the measurements of Ramamonjariosa & Mollo-Christensen (1979, figure 3*e*) that this effect continues at least to the third harmonic. Thus the localization of ak in the fundamental band leads to a further enhancement of the *total* wave amplitude as a result of the corresponding localized contributions from the higher-harmonic bands. This localization of ak , which would not be directly evident without measurements of the wavenumber, helps describe the developing asymmetry of the wave groups. These observations are not consistent with the assumption of an approximately constant wavenumber, and demonstrate the importance of considering wavenumber modulations in describing the evolution of the wavetrain.

Next we come to the identification of phase reversals and the concomitant rapid variations in the modulation variables. In one of the earliest papers dealing with the stability of nonlinear deep-water waves, Lighthill (1965) predicted that a singularity would result after a finite time. Subsequently Chu & Mei (1970) showed that, for modulations of finite length, an additional term contributes to the dispersion relationship and suppresses the singularity. These measurements show that regions of very rapid variations in the phase do occur near the minima of wave amplitude. The measurements are unlikely to be very accurate in regions of very rapid phase reversal; however, the changes in phase measured independently at the two gauges are consistent. If they were in significant error across the 'jumps' then the wavenumber would not recover to a value consistent with the frequency in the central region of the group, and this error would accumulate across each jump. This is convincing evidence that these phase jumps are real despite their occurrence in regions of small amplitude.

As far as I am aware, these phase jumps have not been directly observed before, and clearly further measurements need to be made. Perhaps the most important question to be answered concerns their possible role in the shift to lower frequency following wave breaking (Lake *et al.* 1977; Melville 1982). Ramamonjariosa & Mollo-Christensen (1979) have drawn attention to the phenomenon of 'crest pairing' in both laboratory and ocean wind waves. Their description of this is perhaps a little vague ('One crest simply overtakes the previous crest and disappears. As a result a wave of twice the dominant wave period is produced momentarily'); nevertheless, it seems that phase reversals of the kind measured here may be what they saw. The large gradients in phase speed (figure 5*b*) may appear as though one crest overtakes the previous crest. The observation that the frequency is simply halved is not consistent with our measurements, although the trend appears correct. The polar diagram (figure 4*b*), with the orbit not passing around the origin, may be consistent with a crest not appearing in its expected place in the time series; however, it also suggests that 'trough pairing' may be an equally valid name, with the loss of an expected trough. Lake & Yuen (1978) described the downshift qualitatively as a 'loss' of a wave crest in each modulation period when the amplitude appears to be reduced to zero. Their description appears to be qualitatively consistent with our measurements.

I would like to thank Bruce West for introducing me to the communications literature, and my colleagues at the Hydraulics Laboratory of Scripps Institution of Oceanography for their assistance with the experiments. This work was supported by National Science Foundation Grants OCE 77-240005, OCE 80-09461 and MEA 77-17817.

Appendix. Errors

It is not possible to make a very reliable estimate of the errors involved in the measurements reported here; however, we can present convincing arguments that they do not significantly influence the main results reported. The two important sources of error are the deteriorating wave-gauge response with increasing frequency and the finite-difference approximation of the gradients in the phase. The static calibration of the wave gauges typically gives an r.m.s. error in the calibration curve of ± 0.02 cm, so this must be taken as a minimum error. Extrapolating this error to dynamic measurements is not possible but the results provide some checks. For weakly modulated waves the measurements (figure 2*a*) show an error, when compared to the theoretical phase, of at most 1–2%. The slope is only a small correction to the measured phase speed and we expect that most of the error comes from the measured frequency σ and wavenumber k . Thus $\epsilon_\sigma + \epsilon_k \sim 0.02$, where ϵ_σ and ϵ_k are the fractional errors in σ and k respectively. The frequency corresponds to a phase difference $O(10^{-1})$ rad and the wavenumber to a phase difference $O(1)$ rad. So if we assume that independently ϵ_σ or ϵ_k could account for this error we have a maximum phase-difference error $O(10^{-2})$ rad, in the weakly modulated region.

The more serious concern with errors occurs in the region of the phase jumps where the amplitude is small (comparable to the measurement error) and the frequency is large. At first sight this may seem to be a region of rather large errors; however, we expect that the main sources of error in the wave gauges result from film draining behind the receding surface and capillary hysteresis effects in vertical acceleration/deceleration of the surface. The vertical velocity is $O(a\sigma)$ and the vertical acceleration is $O(a\sigma^2)$. The reduction in amplitude in the regions of the phase jumps would appear to compensate for the higher frequency, keeping the errors within acceptable limits. For example, the phases measured *independently* at the two gauges recover across the jumps so that the difference between the measured and computed phase speed is at most about 10% where the higher-order corrections ($\propto a_{xx}$) in the computed phase speeds are expected to be negligible. This implies that while details of the measured phase in these rapidly varying regions may not be accurate the *independently* measured phase jumps may have an error $O(10^{-1})$ rad. It is worth noting that over 7 or so groups shown in figure 5(*b*) this error does not accumulate. This implies that error estimate may be conservative.

In the regions of the phase jumps we do not believe the measurements are quantitatively reliable, especially where the effects of finite gauge separation show up in the average frequency; however, the qualitative features of the measurements appear to be consistent with the computed phase speeds, especially in the 'weaker' events in figure 5(*b*).

REFERENCES

- BRACEWELL, R. N. 1978 *The Fourier Transform and Its Applications*. McGraw-Hill.
 CHU, V. H. & MEI, C. C. 1970 On slowly varying Stokes waves. *J. Fluid Mech.* **41**, 873–887.
 CRAWFORD, D. R., LAKE, B. M., SAFFMAN, P. G. & YUEN, H. C. 1981 Effects of nonlinearity and spectral bandwidth on the dispersion relation and component phase speeds of surface gravity waves. *J. Fluid Mech.* **112**, 1–32.

- DEUTSCH, R. 1962 *Nonlinear Transformations of Random Processes*. Prentice-Hall.
- FEIR, J. E. 1967 Discussion: Some results from wave pulse experiments. *Proc. R. Soc. Lond.* **A299**, 54–58.
- LAKE, B. M. & YUEN, H. C. 1978 A new model for nonlinear wind waves. Part 1: Physical model and experimental evidence. *J. Fluid Mech.* **88**, 33–62.
- LAKE, B. M., YUEN, H. C., RUNGALDIER, H. & FERGUSON, W. E. 1977 Nonlinear deep-water waves: theory and experiment. Part 2. Evolution of a continuous wave train. *J. Fluid Mech.* **83**, 49–74.
- LIGHTHILL, M. J. 1965 Contributions to the theory of waves in nonlinear dispersive systems. *J. Inst. Maths Applics* **1**, 269–306.
- LIGHTHILL, M. J. 1967 Some special cases treated by the Whitham theory. *Proc. R. Soc. Lond.* **A299**, 28–53.
- LONGUET-HIGGINS, M. S. 1978*a* The instabilities of gravity waves of finite amplitude in deep water I. Superharmonics. *Proc. R. Soc. Lond.* **A360**, 471–488.
- LONGUET-HIGGINS, M. S. 1978*b* The instabilities of gravity waves of finite amplitude in deep water II. Subharmonics. *Proc. R. Soc. Lond.* **A360**, 489–505.
- LONGUET-HIGGINS, M. S. 1980 Modulation of the amplitude of steep wind waves. *J. Fluid Mech.* **99**, 705–713.
- MELVILLE, W. K. 1981 The instabilities of deep-water gravity waves. In *Proc. IUCRM Symp. on Wave Dynamics and Radio Probing of the Ocean Surface, Miami Beach, May 1981* (to be published).
- MELVILLE, W. K. 1982 The instability and breaking of deep-water waves. *J. Fluid Mech.* **115**, 165–185.
- PHILLIPS, O. M. 1981*a* Wave interactions – the evolution of an idea. *J. Fluid Mech.* **106**, 215–227.
- PHILLIPS, O. M. 1981*b* The dispersion of short wavelets in the presence of a dominant long wave. *J. Fluid Mech.* **107**, 465–485.
- RAMAMONJIARISOA, A. 1974 Contribution a l'étude de la structure statistique et des mécanismes de génération des vagues de vent. Thèse de doctorat d'état, Inst. de Mécanique Statistique de la Turbulence, Université de Provence.
- RAMAMONJIARISOA, A. & MOLLO-CHRISTENSEN, E. 1979 Modulation characteristics of sea surface waves. *J. Geophys. Res.* **84**, 7769–7775.
- SAHAR, G. 1981 Modulation of sea surface waves: observations and processing methods. M.S. thesis, M.I.T.
- SCHWARTZ, M., BENNETT, W. R. & STEIN, S. 1966 *Communications Systems and Techniques*. McGraw-Hill.
- WHITHAM, G. B. 1965 Non-linear dispersive waves. *Proc. R. Soc. Lond.* **A283**, 238–261.
- WHITHAM, G. B. 1974 *Linear and Nonlinear Waves*. Academic.